Skelton and A. H. White, *J. Chem. Soc. Dalton Trans.*, 497 (1988).

17. G. A. Lawrance, M. Rossignoli, B. W. Skelton, and A.

H. White, *Aust. J. Chem.*, 40, 1441 (1987).

18. T. H. Lu, H. Y. Kao, C. H. Len, and C. S. Chung, *Acta Cryst.*, C45, 13 (1989).

The Hydrogen Atom in Interstices of Pd Cluster

Keun Woo Lee and Hojing Kim*

Department of Chemistry, Seoul National University, Seoul 151-742
Research Institute for Basic Sciences, Seoul National University, Seoul 151-742
Received January 15, 1992

The electronic structure change caused by insertion of hydrogen into the interstices of Pd cluster is studied. Several properties such as energy, reduced overlap population (ROP), electon density (ED) and density of states (DOS) are calculated by Extended Hückel Method. Various types of clusters are considered. The same is performed on Ni and Pt and all the results are compared. The results show that the hydrogen atom in Pd is stabilized remarkably but its wave function is almost unperturbed. The fact is compatible with noticeable solubility of hydrogen in Pd but may not be a positive enough evidence to rationalize the claimed cold fusion phenomenon. It is also found that a remarkable charge transfer from Pd atom to hydrogen atom occurs.

Introduction

Pons and Fleishmann reported an unusual phenomenon[1] that the fusion reaction can occur at room temperature by the electrochemical method. Its reproducibility[2] and other related study such as physical and chemical investigations[3-16] of Palladium-Hydrogen (Pd-H) systems have reported. Quantum mechanical and theoretical calculations for simple Pd cluster were also performed[17-25]. In fact, the concern for metal-hydrogen system[26-28] began about a century ago[29] and high solubility of hydrogen in Pd has caused keen interests in Pd-H system[30-78].

The aim of this study is to assess the electronic structure change caused by insertion of hydrogen into Pd. The question is of statics that 'How hydrogen exists in Pd' rather than of dynamics that 'How hydrogen enters Pd'. Scanning tunneling microscope (STM)[79-81] has presented photographs for metals[82-88], including Pd, which reveal the extreme roughness of these surfaces. As most electrochemical reactions occur in these rough surfaces, it is reasonable to regard this phenomenon as a reaction between small Pd cluster and hydrogen. Therefore, here, it seems that the molecular orbital (MO) calculation is more appropriate than band calculation[89]. Christensen[23] and Lohr[24] have reported that the hydrogen would exist as atomic entity in Pd. So we assume that the hyrogen exists as atomic form in the interstice of the Pd cluster. This article is divided into three parts as follows.

Part I. The electronic structure of atomic hydrogen perturbed by crystal field potential[90,91] is studied by variational method. Six Pd atoms are arrayed to form an octahedron and each atom is regarded as a point charge. A hydrogen atom is put into the center of the octahedron, and then its energy and eigenstate are computed. The same is performed on the hydrogen atom in a tetrahedral field.

Part II. A face centered cubic cluster of 44 Pd atoms, with 19 octahedral and 32 tetrahedral interstices, is constructed. After inserting hydrogen atoms into the interstices of the cluster, the energy and electronic structure of the system are studied by Extended Hückel method[92-94].

Part III. The clusters of Ni and Pt are compared with that of Pd. The f.c.c. clusters of 32 metal and 32 hydrogen atoms are constructed, respectively, and then they are interwoven to form an NaCl-like structure. The systems are studied as in part II and the difference of the results for three metal are analysed.

Definitions of quantities used throughout the text are given in appendix.

Calculation and Results

Part 1. Perturbation on Hydrogen Atom Located in Octahedral and Tetrahedral Potential.

A hydrogen atom is at the center of 6 or 4 charge field as shown in Figure 1. The field is of the cubic symmetry. This is one of the simple model potential which a hydrogen atom would experience when it is located at the center of octahedral or tetrahedral interstices of Pd. In fact, if the distance of Pd-H is large enough, the interaction between two atoms would be of purely electrostatic nature.

Total Hamiltonian of the system under the octahedral field can be written as

$$H = H_0 + V_{O_h} \tag{1}$$

where H_0 is the total Hamiltonian of isolated hydrogen atom and V_{O_h} is perturbation from 6 point charges. Using atomic unit, each term can be expressed as

$$H_0 = -\nabla^2/2 - 1/r \tag{2}$$
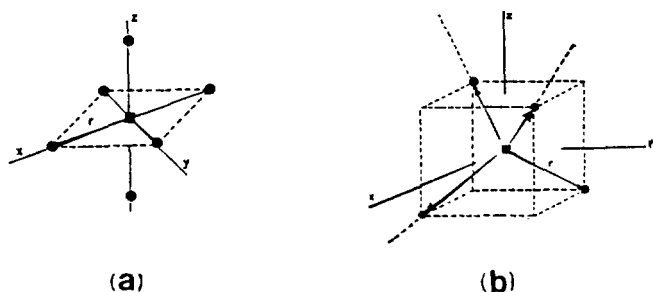
(a)   **(b)**

Figure 1. The cluster model used in part I. Solid circles and squares represent positions of metal and hydrogen atom. Pd-H distance, r, is 1.95 Å in (a) and 1.69 Å in (b).

$$V_{O_h} = -\zeta \sum_{k=1}^{6} \frac{1}{|r-r_k|} \qquad (3)$$

where r_k is th position of each Pd atom, and ζ is the point charge which represents the effect of ligand Pd atom. We take ζ as 1.5 which corresponds to, according to the Slater's rule, the exponent of 5s of Pd. V_{O_h}, a multi-centered potential, can be expanded by Legendre addition theorem[95]:

$$V_{O_h} = -12 \cdot (\pi)^{1/2} \zeta \, r_>^{-1} \, Y_{00}$$

$$- (7/3) \cdot (\pi)^{1/2} \zeta \, (r_<^4/r_>^5)[Y_{40} + (5/14)^{1/2}(Y_{44} + Y_{4,-4})]$$

$$- (3/2) \cdot (\pi/13)^{1/2} \zeta \, (r_<^6/r_>^7)[Y_{60} - (7/2)^{1/2}(Y_{64} + Y_{6,-4})]$$

$$- \cdots\cdots \qquad (4)$$

Likewise, V_{T_d} is expressed by

$$V_{T_d} = -8 \cdot (\pi)^{1/2} \zeta \, r_>^{-1} \, Y_{00}$$

$$- (28/27) \cdot (\pi)^{1/2} \zeta \, (r_<^4/r_>^5)[Y_{40} + (5/14)^{1/2}(Y_{44} + Y_{4,-4})]$$

$$- (16/9) \cdot (\pi/13)^{1/2} \zeta \, (r_<^6/r_>^7)[Y_{60} - (7/2)^{1/2}(Y_{64} + Y_{6,-4})]$$

$$- \cdots\cdots \qquad (5)$$

Here, $r_>$ and $r_<$ are defined by

$$r_> = |r|, \quad r_< = |r_k| \quad \text{for} \quad |r| > |r_k|$$

and

$$r_< = |r|, \quad r_> = |r_k| \quad \text{for} \quad |r| < |r_k|,$$

and the Y_{lm} represents spherical harmonics[95]. Since the magnitudes of two successive terms of Eq. (4) and (5) differ approximately by order of 1 or 2, the fourth and higher terms may be ignored.

The atomic orbitals (AO's) which contribute significantly to the first order perturbation function are selected as bases. That is, 19 atomic orbitals (1s, 2s, ..., 7s, 5g_{-4}, 5g_0, 5g_{+4}, 6g_{-4}, 6g_0, 6g_{+4}, 7g_{-4}, 7g_0, 7g_{+4}, 7i_{-4}, 7i_0, 7i_{+4}) are taken. Ground state energy and wavefunctions are listed in Table 1.

In the case of octahedral potential, the ground state energy of hydrogen (−0.5 a.u.) is stabilized to −2.9344 a.u. (−2.3661 for tetrahedral potential) and the coefficient of 1s orbital is 0.9988 (0.9979 for tetrahedral potential). The latter means the ground state MO of this system is almost equal to 1s orbital os isolated hydrogen atom.

To estimate higher order correction, the basis functions are expanded to 140 atomic orbitals, all AO's from 1s to 7i_{+6} orbital. The result shows no energy improvement (Table

Table 1. Ground State Energy and Wavefunction of Electrostatic Potential System

Potential	Type	$^aO_h(19)$	$^bT_d(19)$	$^aO_h(140)$	$^bT_d(140)$
Energy(eV)		−2.9344	−2.3661	−2.9344	−2.3661
MO	1s	0.9988	0.9979	0.9988	0.9979
coefficient[d]	2s	0.0465	0.0589	0.0465	0.0589
	3s	0.0148	0.0205	0.0148	0.0205
	4s	0.0076	0.0110	0.0076	0.0110
	5s	0.0048	0.0071	0.0048	0.0071
	6s	0.0034	0.0051	0.0034	0.0051
	7s	0.0025	0.0039	0.0025	0.0039
	5g_{-4}	0.0000	0.0000	0.0000	0.0000
	...				
	...				

[a] Octahedral and [b] tetrahedral potential. [c] Number of basis functions. [d] The seven significant coefficients are shown. The rest are approximately zero.
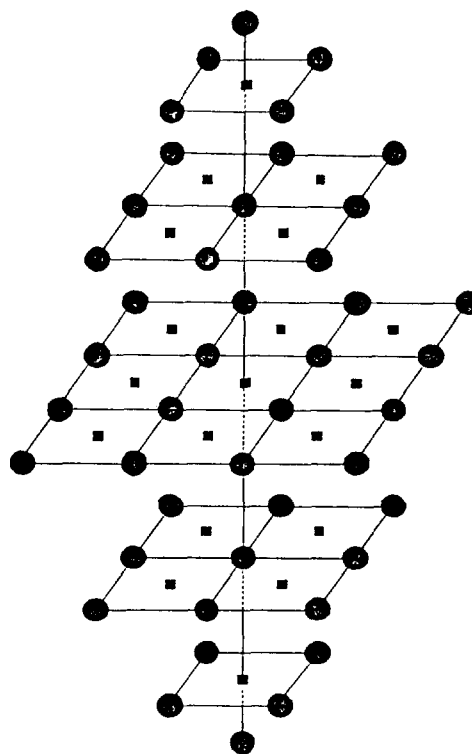

Figure 2. The Pd_{44} cluster. Solid circles and small squares represent 44 Pd atoms and 19 octahedral interstices respectively. The cluster also has 32 tetrahedral interstices (not designated in the figure).

1). That is, the 19 basis functions are sufficient for the practical purpose.

It is found that both the octahedral and tetrahedral potential stabilize the hydrogen atom in its energy, but do not cause the significant change in its electronic structure. The fact is referred in the selection of basis function of hydrogen atom in part II and III.

Part II. Energy and Electronic Structure of Hydrogen Placed in Interstices of F.c.c. Cluster of 44 Pd

Table 2. EHT Parameters for Pd of Pd₄₄ Cluster

	ξ_1	ξ_2	c_1	c_2	H_{ii}^a(eV)
5s	2.190				−7.32
5p	2.152				−3.75
4d	5.983	2.613	0.5264	0.6373	−12.02

Exponent parameters and coefficients are obtained from reference 96. [a] Energy paramerters are obtained from reference 97.

Table 3. Stabilization Energy (S.E.) of Pd₄₄ Cluster

	Pd₄₄H₁₉(O_h) (eV)	Pd₄₄H₃₂(T_d) (eV)
Pd-H clusters	−5630.80	−5859.27
H clusters	−266.89	−475.48
Pd₄₄ cluster	−5300.64	−5300.64
Tatal S.E.	−63.38	−83.15
[a]Unit S.E.	−3.34	−2.60

[a]Obtained from dividing total S.E. by the number of hydrogen atoms.

Atoms

Pd₄₄ cluster in Figure 2 has 19 octahedral and 32 tetrahedral interstices. The cluster has identical shape with the cluster in Figure 1(a) but is of different size. After hydrogen atoms are placed into the interstices of two different kinds, the total energy and reduced overlap population (ROP) are evaluated. It has been reported that if Pd crystal absorbs hydrogen, the lattice parameter of Pd increases by about 6 percent[25]. Nevertheless, frozen geometry is used for the convenience of camparison, since our major concern is the electronic structure change caused by hydrogen insertion. The EHT parameters used here are listed in Table 2.

Energy Stabilization. In EHT formalism, total energy is given as the sum of one electron energies. This is listed in Table 3. It shows that the hydrogen in octahedral interstices is more stable than that in tetrahedral ones. This is compatible with the results of part I.

Reduced Overlap Population (ROP). ROP is evaluated to give a quantitative description of electronic structure and computed values are listed in Table 4.

The part C in Table 4 shows the ROP change caused by hydrogen insertion into the interstices. When two atoms A and B are bound together, one expects in general that the electron density decreases at each atomic site and increases at the internuclear region. The ΔP_{AA}(H) in Table 4C is positive against the expectation. It means the electron densities at the hydrogen sites in Pd crystal are more dense than at those in imaginary hydrogen network. The ΔP_{AA}(Pd), however, shows a large negative value and the ΔP_{AA}(Pd-H) small positive. Namely, the electrons of Pd atoms move into internuclear region of Pd and hydrogen atom for bonding. The fact that all electrons participated in bonding are provided exclusively from Pd atoms signifies the charge transfer from Pd atom to hydrogen atom. It may be understood either as the intrinsic character of Pd atom or as edge effect of the cluster. To elucidate the nature of the charge transfer, Pd is compared with Ni and Pt in Part III.

Table 4. Reduced Overlap Population Obtained from H₁₉, H₃₂, H₅₁ and Pd₄₄ Clusters(A), Three Pd-H Clusters(B), and their Net ROP(C)

		Pd₄₄H₁₉(O_h)	Pd₄₄H₃₂(T_d)	Pd₄₄H₅₁(O_h+T_d)
A	[a]P_{AA}(H)	0.9567	0.8766	0.8411
	P_{AA}(Pd)	9.8317	9.8317	9.8317
	[b]P_{AB}(Pd-Pd)	0.0417	0.0417	0.0417
	P_{AB}(Pd-H)	0.0000	0.0000	−
	P_{AB}(H-H)	0.0091	0.0513	−
B	P_{AA}(H)	0.9861	0.8786	0.8436
	P_{AA}(Pd)	9.5838	9.5155	9.5189
	P_{AB}(Pd-Pd)	0.0318	0.0038	−0.0261
	P_{AB}(Pd-H)	0.1030	0.1393	−
	P_{AB}(H-H)	0.0012	0.0193	−
[c]C	ΔP_{AA}(H)	0.0294	0.0020	0.0025
	ΔP_{AA}(Pd)	−0.2479	−0.3162	−0.3129
	ΔP_{AB}(Pd-Pd)	−0.0099	−0.0379	−0.0678
	ΔP_{AB}(Pd-H)	0.1030	0.1493	−
	ΔP_{AB}(H-H)	−0.0079	−0.0320	−

[a]P_{AA} are averaged values for 44 Pd atom and each hydrogen because it is one atomic value. [b]P_{AB} can not be averaged because it is of interatomic nature, so we take these values at the center of cluster. [c]This sub-table is constructed by B-A.
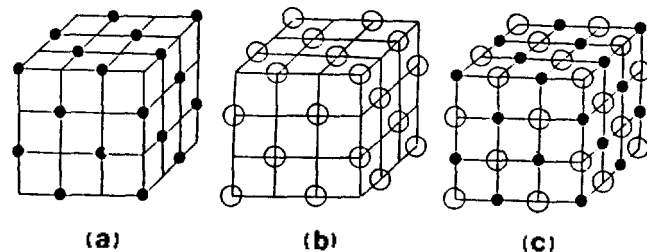
Figure 3. The shape of clusters. (a) H₃₂ cluster (b) M₃₂ cluster (M=Ni, Pd, and Pt) (c) M₃₂H₃₂ cluster.

Table 5. Lattice Parameters

Crystal	Lattice parameter[a](Å)
Ni	3.52
Pd	3.89
Pt	3.92

[a]Obtained from reference 98.

Part III. Comparison of Pd-H Network with Ni-H and Pt-H Networks

The model cluster for the calculation is shown in Figure 3. NaCl-like structure is chosen to make the number of metal atoms equal to that of hydrogen ones. The cluster consists of 32 atoms and of 4 layers. Ni, Pd, and Pt crystals are of f.c.c. and their lattice parameters are listed in Table 5.

Energy parameters are obtained by the charge iteration method for the clusters[92-94] and are listed in Table 6. The total energy, density of states (DOS), electron density (ED), and reduced overlap population (ROP) are evaluated for the clusters.

Table 6. EHT Parameters for Ni, Pd and Pt of M_{32} Cluster

	Orbital	$^aH_{ii}$ (eV)	$^bH_{ii}$ (eV)	$^c\zeta_1$	$^c\zeta_2$	$^cC_1$	$^cC_2$
Ni	4s	−7.91	−8.33	1.925			
	4p	−3.71	−4.10	1.925			
	3d	−10.16	−10.51	5.75	2.20	0.5817	0.5800
	1s(H)	−13.6	−10.92	1.3			
Pd	5s	−6.58	−7.57	2.190			
	5p	−0.29	−1.20	2.152			
	4d	−9.43	−11.13	5.98	2.613	0.5535	0.6701
	1s(H)	−13.6	−10.80	1.3			
Pt	6s	−8.86	−9.38	2.554			
	6p	−4.23	−4.56	2.554			
	5d	−10.67	−11.47	6.013	2.696	0.6336	0.5513
	1s(H)	−13.6	−11.81	1.3			

$^aH_{ii}$ obtained by charge iteration method for metal and ^{b}metal-hydrogen cluster. The charge iteration parameters used above are listed in references 99-101. ^{c}Exponent parameters and coefficients are obtained from references 97, 102 and 103.

Table 7. Cluster Energy Stabilization of M_{32} Clusters

		Ni(eV)	Pd(eV)	Pt(eV)
M-H	molecule	−2.28	−1.08	−2.29
$^aM_{32}H_{32}$	cluster	−3.27	−16.31	−8.77

^{a}Obtained from deviding the total S.E. of each cluster by the number of M-H pairs.

Energy Stabilization. The binding energy of the imaginary M-H molecule (with the internuclear separation of the lattice parameter), and the stabilization energy of $M_{32}H_{32}$ clusters are evaluated, respectively. The latter is divided by 32 for the visual comparison and its result is listed (Table 7).

The imaginary M-H molecule is less stable in M=Pd case than else. However, in the cluster of $M_{32}H_{32}$, an unususal stabilization is seen in M=Pd case. This result seems to be compatible with the high solubility of hydrogen in Pd. The DOS and PDOS and introduced to elucidate the cause of stabilization.

Density of States (DOS) and Projected Density of States (PDOS). As one sees in Figure 4, there is no signal at −14 eV region in DOS of metal cluster[(b)] but small peaks appear in metal-hydrogen ($M_{32}H_{32}$) cluster[(c)]. These peaks are due to bonding orbitals made of d-orbitals of metal and 1s-orbital of hydrogen. And Figure 5 shows that s-band [(a) and (b)] and p-band[(c) and (d)] do not contribute in any significant extent to the states below Fermi energy (ε_F).

The figure shows that the energy stabilization is caused essentially by d-band[(e) and (f)]. The peak center remains almost unchanged for Ni and Pt. But in $Pd_{32}H_{32}$, the peak center of d-band experiences notable dislocation. The d-band shift of $Pd_{32}H_{32}$ contributes to the stabilization of the total system.

Electron Density (ED) and Projected Electron Density (PED). The change of electron density is displayed
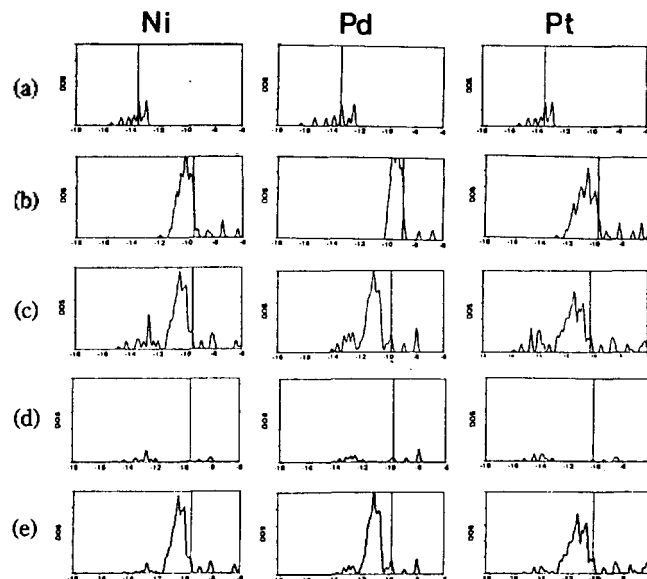

Figure 4. DOS curves of (a) H_{32} cluster, (b) M_{32} cluster and (c) $M_{32}H_{32}$ cluster. PDOS at (d) hydrogen and (e) metal of $M_{32}H_{32}$ cluster. This PDOS represents the contribution of a specific fragment of the system to the total DOS. For all plots, the unit of abscissa is eV and the vertical solid line designates Fermi energy (ε_F).
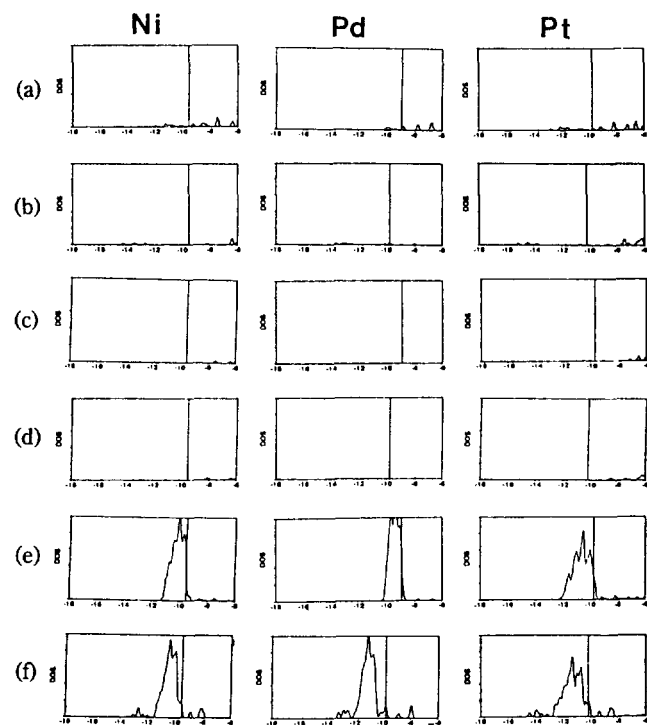

Figure 5. PDOS curves of (a) s-orbitals of metal in M_{32} cluster, (b) s-orbitals of metal in $M_{32}H_{32}$ cluster, (c) p-orbitals of metal in M_{32} cluster, (d) p-orbitals of metal in $M_{32}H_{32}$ cluster, (e) d-orbitals of metal in M_{32} cluster, and (f) d-orbitals of metal in $M_{32}H_{32}$ cluster. It is noticeable that this PDOS represents the contribution of a specific atomic orbital of the system to total DOS. For all plots, the unit of abscissa is eV and the vertical solid line designates Fermi energy (ε_F).
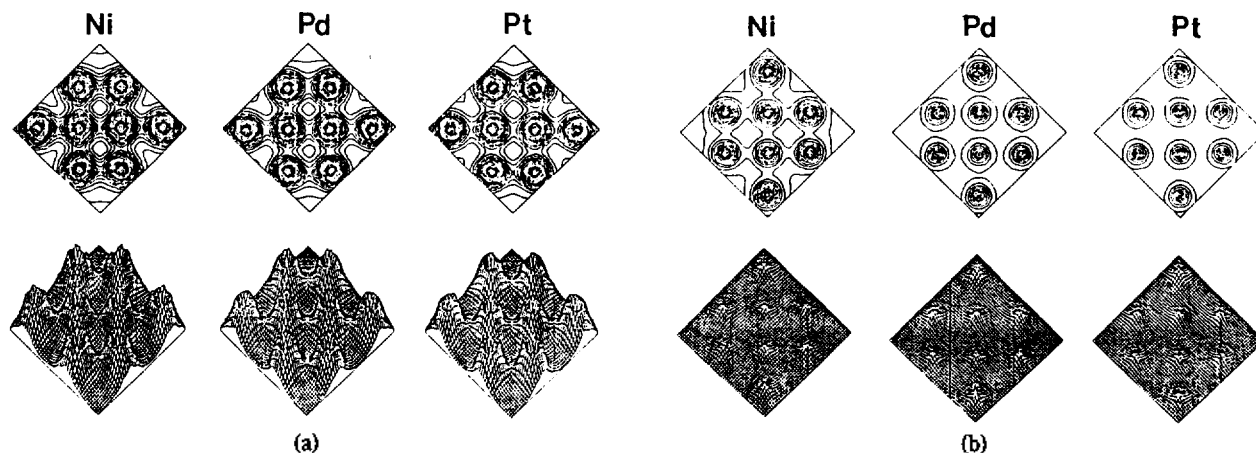
Hydrogen in Pd Cluster

Bull. Korean Chem. Soc., Vol. 13, No. 4, 1992 371

Figure 6. Electron density diagram of (a) M_{32} cluster and of (b) H_{32} cluster.
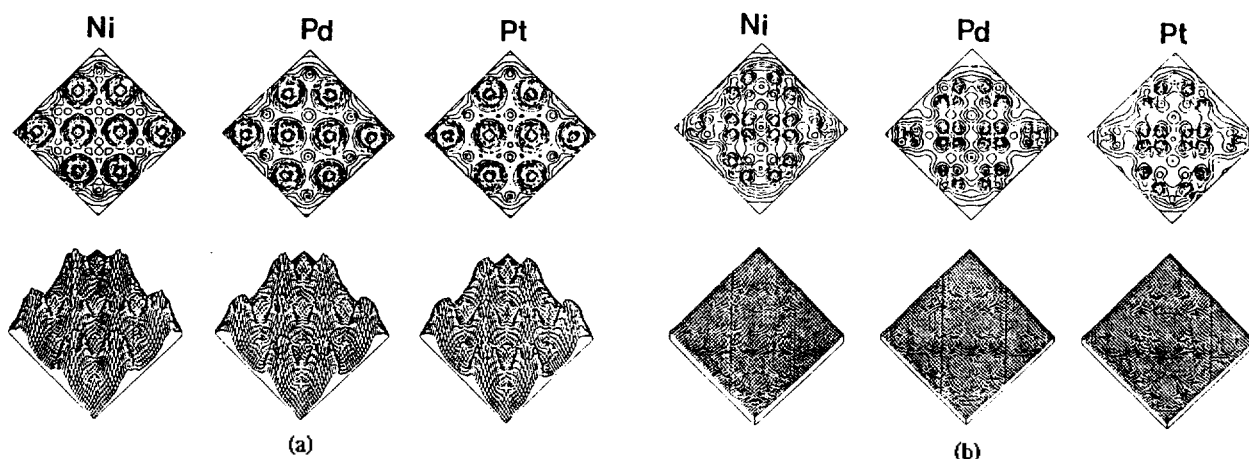

Figure 7. Electron density diagrams of (a) $M_{32}H_{32}$ cluster, and (b) Difference ED diagram ([Fig. 7(a)]-[Fig. 6(a)+Fig. 6(b)]). The diagram shows electron density change after insertion of H_{32} into M_{32} cluster.
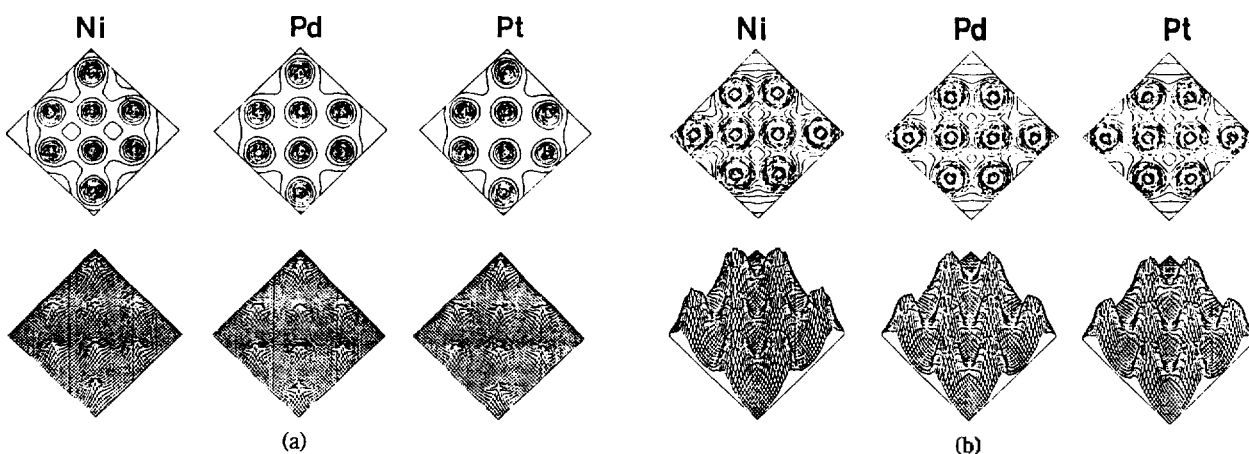

Figure 8. Projected electron density (PED) diagrams for (a) metal and (b) hydrogen from total ED.

in 3-dimensional diagram (Figure 6-9). They are rather qualitative but easily understandable. The quantitative description will be given in ROP table.

In Figure 6. the eight crators in (a) represent electron densities of eight metal atoms placed in third layer from the top of the cluster of Figure 3(a). The center of the crator is the site of metal atom and the eight hills in (b) are at

the sites of hydrogen atoms. The ED diagrams of $M_{32}H_{32}$ clusters are given in Figure 7(a). It is noticeable that the small eight hills still remain.

The electron densities of metal and hydrogen [Figure 6(a) and (b)] are subtracted from those of metal-hydrogen clusters [Figure 7(a)] respectively. The resultant densities [Figure 7(b)] represent ED change caused by formation of me-
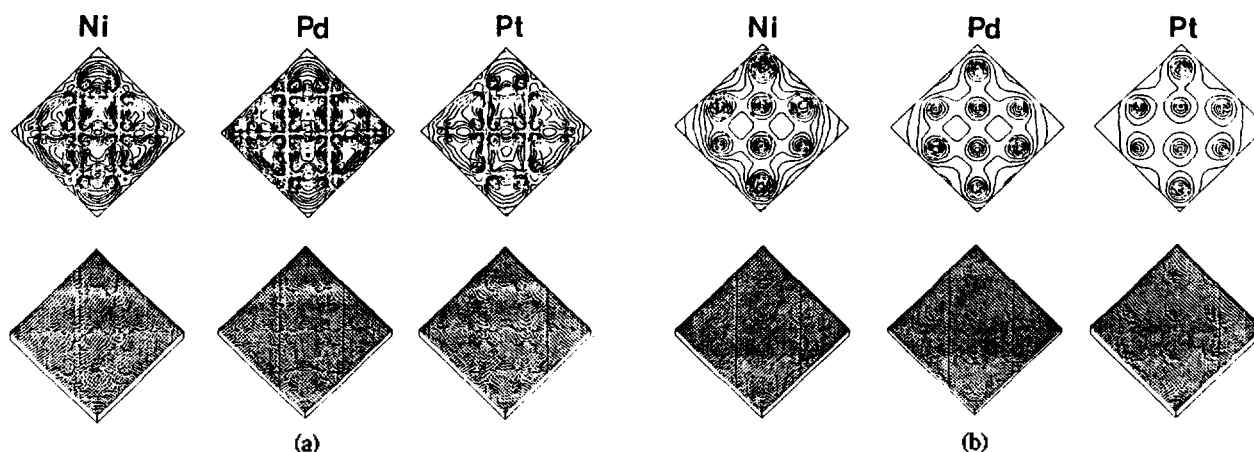
Ni Pd Pt Ni Pd Pt

(a) (b)

Figure 9. Difference PED diagram (a) ([Fig. 8(b)]-[Fig. 6(b)]) (b) ([Fig. 8(a)]-[Fig. 6(a)]). The diagrams show clearly the electron density changes for the metal (a) and hydrogen (b).

Table 8. Reduced Overlap Population Obtained from M_{32} and H_{32} Clusters(A), $M_{32}H_{32}$ Cluster(B), and their Net ROP(C)

		Ni	Pd	Pt
A	$^{a}P_{AA}$(H)	.9364	.9571	.9591
	P_{AA}(M)	9.6018	9.8578	9.5049
	$^{b}P_{AB}$(M-H)	.0770	.0294	.1079
	P_{AB}(M-H)	.0000	.0000	.0000
	P_{AB}(H-H)	.0198	.0131	.0116
B	P_{AA}(H)	.7488	.8660	.7516
	P_{AA}(M)	9.3972	9.5923	9.3604
	P_{AB}(M-M)	.0694	.0141	.0906
	P_{AB}(M-H)	.1306	.0912	.1198
	P_{AB}(H-H)	.0004	.0023	.0000
^{c}C	ΔP_{AA}(H)	−.1877	−.0911	−.2075
	ΔP_{AA}(M)	−.2046	−.2655	−.1445
	ΔP_{AB}(M-M)	−.0076	−.0153	−.0173
	ΔP_{AB}(M-H)	.1306	.0912	.1198
	ΔP_{AB}(H-H)	−.0194	−.0108	−.0116

$^{a}P_{AA}$ are averaged-values for 32 metal atoms and 32 hydrogen atoms. $^{b}P_{AB}$ can not be averaged because it is interatomic nature, so we take these values at the center of cluster like Pd_{44} cluster case. ^{c}This sub-table is costructed by B-A.

tal-hydrogen cluster. The diagram shows all the atomic sites are collapsed. It means that the electrons of each atoms are spent for the bond formation. The shape of collapsed area looks like that of $d(x^2-y^2)$-orbital. That is, the electrons from metal $d(x^2-y^2)$-orbital contribute to binding. Since the $d(x^2-y^2)$ and $d(z^2)$ orbitals of metal atom belong to same symmetry (e_g), $d(z^2)$ orbital interacts with $1s$ orbital of the hydrogen atom likewise.

Figure 8 is the PED diagrams of hydrogen [(a)] and metal [(b)] made from the total density [Figure 7(a)]. The ED of Figure 6 is subtracted from that of Figure 8 (namely, Difference PED) and the result is drawn in Figure 9. If the ED changes do not occur in the process of the formation

of the interwoven network, $M_{32}H_{32}$, from the networks M_{32} and H_{32}, then it will be flat.

In reality, however, the result is otherwise. Figure (a) shows that $d(x^2-y^2)$ (and $d(z^2)$) orbitals of metal contribute to the bond. The extremely small contribution of hydrogen to the bond is also shown in (b). It should be noted that the shape of the diagram for M=Pd case. In (a), it shows rather deep holes at the sites of Pd atoms, and nearly flat plane in (b). That is, in comparison with hydrogen atom, overwhelmingly large portion of electrons needed for the Pd-H bond formation is supplied by Pd atoms. So, it seems that hydrogen atom in Pd cluster keeps its electronic structural identity to almost unperturbed. The quantitative aspect of this will be unveiled in following ROP calculation (Table 8C).

Reduced Overlap Population (ROP). The ROP are listed in Table 8. The P_{AA}(H) in A are almost equivalent for three metal clusters. But in B, the values for Ni and Pt are about 0.75 and for Pd is 0.87. That is, the hydrogens in Pd cluster lose their electrons less than in Ni and Pt clusters.

The net ROP, ΔP, which manifests ROP change after insertion of hydrogen into the metal is given in Table 8C. ΔP_{AA}(H), ΔP_{AA}(M) and ΔP_{AB}(M-H) show change of the electron population for the formation of metal-hydrogen cluster. The data signifies that the Ni-H and Pt-H bonds are more covalent and the Pd-H bond is comparatively more ionic. That is, charge transfer from Pd atom to hydrogen atom occurs. This is consistent with Tománek's report[25].

Conclusion

In part I, it was found that a hydrogen atom in the point charge field is remarkably stabilized but its wave function remains nearly unperturbed. We have performed more advanced calculations in part II but obtained qualitatively similar results. Because Extended Hückel method is based upon MO theory, the concept of bond is introduced naturally. In the case of Pd-H bond, the charge transfer from Pd atom to hydrogen atom is remarkable. It may be understood as the intrinsic character of Pd atom or may be interpreted as the edge effect of the cluster. In order to clarify the ques-

tion, the comparison with other metal clusters are made in part III. The same methodology used in part II is also applied in part III. The result shows that only the hydrogen in Pd is stabilized due to the shift of the Pd d-band. Thus it confirms that the charge transfer is definitely of the intrinsic character of Pd atom.

In summary, the hydrogen atom in Pd is stabilized energetically but its wave function is almost unperturbed. The result is compatible with notable solublity of hydrogen in Pd. But we do not find any positive enough evidence to rationalize the claimed cold fusion phenomenon[1], where hydrogen atom in Pd would experience definitely serious perturbation[104-109].

Appendix

1. Density of States (DOS) and Projected Density of States (PDOS)

$$\rho(E)=\sum_k \delta(E-\varepsilon_k) \quad \text{(DOS for bulk)}$$

$$\rho_i(E)=\sum_k |c_{ik}|^2 \delta(E-\varepsilon_k) \quad \text{(PDOS for bulk)}$$

$$\rho^c(E)=(2\pi\sigma^2)^{-1/2}\sum_k \exp[-(E-\varepsilon_k)^2/2\sigma^2] \quad \text{(DOS for cluster)}$$

$$\rho_i^c(E)=(2\pi\sigma^2)^{-1/2}\sum_k |c_{ik}|^2 \exp[-(E-\varepsilon_k)^2/2\sigma^2]$$

$$\text{(PDOS for cluster)}$$

2. Electron Density (ED) and Projected Electron Density (PED)

ED of isolated fragment A

$$\Gamma^A(r)=\sum_i f_i^*(r) \; n_i^A f_i(r) \qquad f_i= \sum_{k\in A} \phi_k A_{ki}$$

$$= \sum_{i\in A} \sum_{j\in A} \sum_k n_k^A A_{ki}^* Q_{ij}(r)A_{jk} \;, \; Q_{ij}=\phi_i^*\phi_j$$

ED of A-B composite system

$$\Gamma^T(r)=\sum_k \Psi_k^*(r) \; n_k \Psi_k(r) \quad, \; \Psi_k=\sum_i \phi_i C_{ik}$$

$$=\sum_k n_k \sum_i \sum_j C_{ki}^* Q_{ij}(r)C_{jk}$$

$$= \sum_{i\in A} \sum_k n_k \sum_j C_{ki}^* Q_{ij}(r)C_{jk}+ \sum_{i\in B} \sum_k n_k \sum_j C_{ki}^* Q_{ij}(r)C_{jk}$$

$$=\Gamma^{T-A}(r)+\Gamma^{T-B}(r)$$

PED of fragment A in A-B composite system

$$\Gamma^{T-A}(r)= \sum_{i\in A} \sum_k n_k \sum_j C_{ki}^* Q_{ij}(r)C_{jk}$$

3. Reduced Overlap Population (ROP)

$$P_{AA}= \sum_{i\in A} \sum_k n_k C_{ki}^2$$

$$P_{AB}=2 \sum_{i\in A} \sum_{j\in B} \sum_k n_k C_{ki}^* S_{ij} C_{jk}, \; S_{ij}: \text{overlap matrix}$$

References

1. M. Fleishmann and S. Pons, *J. Electroanal. Chem.*, **261**, 301 (1989).

2. S. E. Jones, E. P. Palmer, J. B. Czirr, D. L. Decker, G. L. Jensen, J. M. Thorne, S. F. Taylor, and J. Rafelski, *Nature* **338**, 737 (1989).

3. H. Chen, N. E. Brener, and J. Callaway, *Phys. Rev. B*, **40** (3), 1443 (1989).

4. F. Marchesoni, C. Presilla, and F. Sacchetti, *Europhys. Lett.* **10**(5), 493 (1989).

5. S. Fujita, *Phys. Status Solidi B*, **156**(1), K17 (1989).

6. J. F. Ziegler, T. H. Zabel, J. J. Cuomo, V. A. Gargill III, E. J. Sullivan, and A. D. Marwick, *Phys. Rev. Lett.*, **62**(25), 2929 (1989).

7. J. W. Mintmire, B. I. Dunlap, D. W. Brenner, R. C. Mowrey, H. D. Ladouceur, P. P. Schmidt, C. T. White, and W. E. O'Grady, *Phys. Lett. A*, **138**(1), 51 (1989).

8. T. Bressani, E. Del Giudice, and G. Preparata, *Nuovo Cimento Soc. Ital. Fis. A*, **101**A(5), 845 (1989).

9. G. Horanyi, *Electronchim. Acta* **34**(6), 889 (1989).

10. C. J. Benesh, and J. P. Vary, *Phys. Rev. C. Nucl. Phys.*, **40**(2), R495 (1989).

11. M. Gai, S. L. Rugari, R. H. France, B. J. Lund, Z. Zhao, A. J. Davenport, H. S. Isaacs, and K. G. Lynn, *Nature (London)* **340**, 29 (1989).

12. N. S. Lewis, C. A. Barnes, M. J. Heben, A. Kumer, S. R. Lunt, G. E. McManis, G. M. Miskelly, R. M. Penner, and M. J. Sailor, *Nature(London)*, **340**, 525 (1989).

13. K. H. Johnson and D. P. Clougherty, *Mod. Phys. Lett. B*, **3**(10), 795 (1989).

14. C. W. Chu, Y. Y. Xue, R. L. Meng, P. H. Hor, Z. J. Huang, and L. Gao, *Mod. Phys. Lett. B*, **3**(10), 753 (1989).

15. J. C. Horowitz, *Phys. Rev. C. Nucl. Phys.* **40**(4), R1555 (1989).

16. G. Kreysa, G. Marx, and W. Plieth, *J. Electroanal. Chem. Interfacial Electrochem.*, **266**(2), 437 (1989).

17. W. Schommers and C. Politis, *Mod. Phys. Lett. B*, **3**(8), 597 (1989).

18. M. Apostol and I. A. Dorobantu, *Rev. Roum. Phys.*, **34**(2), 233 (1989).

19. A. Burrows, *Phys. Rev. B*, **40**(5), 3405 (1989).

20. Z. Sun and D. Tomànek, *Phys. Rev. Lett.*, **63**(1), 59 (1989).

21. D. P. Min, *New Phys.(Kor. Phys. Soc.)*, **29**(2), 233 (1989).

22. X. W. Wang, S. G. Louie, and M. L. Cohen, *Phys. Rev. B*, **40**(8), 5822 (1989).

23. O. B. Christensen, P. D. Ditlevsen, K. W. Jacobson, P. Stoltze, O. H. Nielsen, and J. K. Nørskov, *Phys. Rev. B*, **40**(3), 1993 (1989).

24. L. L. Lohr, *J. Phys. Chem.* **93**, 4697 (1989).

25. D. Tomànek, Z. Sun, and S. G. Louie, *Phys. Rev. B*, **43**(6), 4699 (1991).

26. F. A. Lewis, *Platinum Met. Rev.*, **26**, 20, 70, 121 (1982).

27. E. Wicke and H. Broodowsky, *"Hydrogen in Metals"* edited by G. Alefeld and J. Völkl (Springer, Berlin, 1978), Vol. 2, p. 73.

28. F. A. Lewis, *"The Palladium Hydrogen System"* (Academic, New York, 1967).

29. T. Graham, *Philos. Trans. R. Soc. London*, **156**, 399 (1866).

30. A. Sievert and G. Zapf, *Z. Phys. Chem.*, **174**A, 359 (1935).

31. A. Sievert and W. Danz, *Z. Phys. Chem.*, **38**B, 46 (1937).

32. H. Brodowsky and E. Poeschel, *Z. Phys. Chem.*, **44**, 143

(1965).

33. G. Sicking, Z. *Phys. Chem. (Wiesbaden)*, **116**, 63 (1979).
34. T. B. Flanagan and T. Kuji, Z. *Phys. Chem. (Munich)*, **143**, 61 (1985).
35. R. Fromageau and A. Magnouche, Z. *Phys. Chem. (Munich)*, **145**(1), 269 (1985).
36. Y. Sakamoto, Y. Tanaka, K. Baba, and T. B. Flanagan, Z. *Phys. Chem. (Munich)*, **158**(2), 237 (1988).
37. L. J. Gillispie and W. R. Downs, *J. Am. Chem. Soc.*, **61**, 2496 (1939).
38. J. B. Condon, *J. Phys. Chem.*, **79**(1), 42 (1975).
39. G. L. Powell, *J. Phys. Chem.*, **80**(4), 375 (1976).
40. G. L. Powell, *J. Phys. Chem.*, **83**(5), 605 (1979).
41. Y. Ebisuzaki, W. J. Kass, and M. O'Keeffe, *J. Chem. Phys.*, **46**(4), 1378 (1967).
42. S. A. Steward, *J. Chem. Phys.*, **63**(2), 975 (1975).
43. G. Boureau, O. J. Kleppa, and P. Dantzer, *J. Chem. Phys.*, **64**, 5247 (1976).
44. G. Boureau and O. J. Kleppa, *J. Chem. Phys.*, **65**, 3915 (1976).
45. E. Wicke and G. Nernst, *Ber. Bunsenges. Phys. Chem.*, **68**, 224 (1964).
46. H. Frieske and E. Wicke, *Ber. Bunsenges. Phys. Chem.*, **77**, 48 (1973).
47. W. R. Tyson, *J. Less-Common Met.*, **70**(2), 209 (1980).
48. Y. Sakamoto, T. Ohishi, E. Kumashiro, and K. Takao, *J. Less-Common Met.*, **88**(2), 379 (1982).
49. Y. Sakamoto, S. Hirata, and H. Nishikawa, *J. Less-Common Met.*, **88**(2), 387 (1982).
50. H. Zuechner and H. G. Schoeneich, *J. Less-Common Met.*, **101**, 363 (1984).
51. D. A. Smith, L. P. Jones, and I. R. Harris, *J. Less-Common Met.*, **103**(1), 33 (1984).
52. M. Doyle, R. C. J. Wileman, and I. R. Harris, *J. Less-Common Met.*, **130**, 79 (1987).
53. R. Lässer and G. L. Powell, *J. Less-Common Met.*, **130**, 387 (1987).
54. R. Lässer, *Phys. Rev. B: Condens. Matter*, **26**, 3517 (1982).
55. R. Lässer and K. H. Klatt, *Phys. Rev. B: Condens. Matter*, **28**(2), 748 (1983).
56. R. Lässer, *Phys. Rev. B: Condens. Matter*, **29**(8), 4765 (1984).
57. S. Möhlecke, C. F. Majkrzak and M. Strongin, *Phys. Rev. B: Condens. Matter* **31**(10), 578 (1986).
58. R. Lässer and G. L. Powell, *Phys. Rev. B: Condens. Matter*, **34**(2), 578 (1986).
59. R. Kirchheim, *Acta Metall.*, **30**(6), 1069 (1982).
60. R. Kirchheim and J. P. Hirth, *Acta Metall.*, **35**(12), 2899 (1987).
61. H. Takeshita and R. B. Mclellan, *Scr. Metall.*, **18**(9), 973 (1984).
62. A. Craft, R. Foley, B. Flanagan, K. Baba, Y. Niki, and Y. Sakamoto, *Scr. Metall.*, **22**(4), 511 (1988).
63. D. Clewley, T. Curran, T. B. Flanagan, and W. A. Oates, *J. Chem. Soc. Faraday Trans.*, **169**, 449 (1973).
64. T. B. Flanagan and J. D. Clewley, *Solid State Commun.*, **31**(11), 865 (1982).
65. R. V. Bucur and V. Mecea *Surf. Coat. Technol.*, **28**(3), 387 (1986).
66. R. V. Bucur, *J. Meter. Sci.*, **22**(9), 3402 (1987).

67. R. Kirchheim, *Prg. Mater. Sci.*, **32**(4), 261 (1988).
68. S. M. Lee and J. Y. Lee, *J. Appl. Phys.*, **63**(9), 4758 (1988).
69. Y. Sakamoto, K. Kajihara, Y. Fukusaki, and T. B. Flanagan, Z. *Phys. Chem. (Munich)*, **159**(1), 61 (1989).
70. S. Ramaprabhu, R. Leiberich, and A. Weiss, Z. *Phys. Chem. (Munich)*, **161**(1), 83 (1989).
71. M. L. Doyle and I. R. Harris, Z. *Phys. Chem. (Munich)*, **163**(1), 59 (1989).
72. G. L. Powell, W. E. Lever, and R. Lässer, Z. *Phys. Chem. (Munich)*, **163**(3), 47 (1989).
73. R. C. J. Wileman, M. Doyle, and I. R. Harris, Z. *Phys. Chem. (Munich)*, **164**(1), 797 (1989).
74. Y. Sakamoto, K. Kajihara, E. Ono, K. Baba, and T. B. Flanagan, Z. *Phys. Chem. (Munich)* **165**(1), 67 (1989).
75. R. V. Bucur, *Scr. Metall.*, **23**(1), 91 (1989).
76. R. Lässer and G. L. Powell, *Fusion Technol.*, **14**(2), 695 (1989).
77. S. Ramaprabhu, N. Rajalakshmi, and A. Weiss, *Ber. Bunsen-Ges. Phys. Chem.*, **93**(6), 686 (1989).
78. H. Shahani and L. Wictorin, *Scand. J. Metall.*, **18**(4), 211 (1989).
79. G. Binnig, H. Roher, Ch. Gerber, and E. Weibel, *Phys. Rev. Letters*, **49**, 57 (1982).
80. G. Binnig and H. Roher, *Surf. Sci.*, **126**, 236 (1983).
81. G. Binnig and H. Roher, *Surf. Sci.*, **152/153**, 17 (1985).
82. A. J. Brunner, A. Stemmer, L. Rosenthaler, R. Wiesendanger, M. Ringger, P. Oelhafer, H. Rudin, and H. J. Güntherodt, *Surf. Sci.*, **181**, 313 (1987).
83. J. O. Besenhard, U. Krebber, J. K. H. Hörber, N. Kanani, and H. Meyer, *J. Electrochem. Soc.*, **136**(12), 3608 (1989).
84. J. E. Demuth, R. J. Hamers, R. M. Tromp, and M. E. Welland, *IBM J. Res. Develop.*, **30**(4), 396 (1986).
85. W. Hösler, R. J. Behm, and E. Ritter, *IBM J. Res. Develop.*, **30**(4), 403 (1986).
86. M. Ringger, B. W. Corb, H. R. Hidber, R. Schlögl, R. Wiesendanger, A. Stemmer, L. Rosenthaler, A. J. Brunner, P. C. Oelhafen, and H. J. Güntherodt, *IBM J. Res. Develop.*, **30**(5), 500 (1986).
87. H. van Kempen and G. F. A. van de Walle, *IBM J. Res. Develop.*, **30**(5), 509 (1986).
88. Th. Berghaus, H. Neddermeyer, and St. Tosch, *IBM J. Res. Develop.*, **30**(5), 520 (1986).
89. T. N. Rhodin and G. Ertl. *"The Nature of the Surface Chemical Bond"* (North-Holland, Amsterdam, 1984).
90. T. M. Dunn, D. S. McClure, and R. G. Pearson, *"Some Aspects of Crystal Field Theory"* (Harper & Row, New York and John WeatherHill, Tokyo, 1965).
91. C. J. Ballhausen *"Introduction to Ligand Field Theory"* (McGraw-Hill, New York, 1962).
92. R. Hoffman, *J. Chem. Phys.*, **39**, 1397 (1963).
93. J. H. Ammeter, H. B. Bürgi, J. C. Thibeault, and R. Hoffman, *J. Am. Chem. Soc.*, **100**, 3686 (1978).
94. M. H. Whangbo and R. Hoffman, *J. Chem. Phys.*, **68**, 5498 (1978).
95. P. M. Morse and H. Feshbach, *"Methods of Theoritical Physics"* (McGraw-Hill New York, 1953).
96. H. Basch and H. B. Gray, *Theor. Chim. Acta*, **4**, 367 (1966).
97. K. Tasmi, R. Hoffmann, A. Yamamoto, and J. K. Skill, *Bull. Jpn. Chem. Soc.*, **54**, 1857 (1981).
98. C. Kittel, *"Introduction to Solid State Physics"* (John Wi-

Synthesis and Structure of Spiro Orthocarbonates

Bull. Korean Chem. Soc., Vol. 13, No. 4, 1992 375

ley & Sons, Inc., New York, 1986).

99. C. J. Ballhausen and H. B. Gray, "*Molecular Orbital Theory*" (W. A. Benjamin, Inc., New York, 1964).

100. V. I. Baranovskii and A. B. Nikolskii, *Theor. Eksp. Khim.*, 3, 527 (1967).

101. D. A. Brown and A. Owens, *Inorg. Chimica Acta*, 5, 675 (1971).

102. J. W. Richardson, W. C. Nieuwpoott, R. R. Powell, and W. F. Edgell, *J. Chem. Phys.*, 36, 1057 (1962).

103. G. Casalone, F. Merati, and G. F. Tantardini, *Chem. Phys. Lett.*, 137(3), 234 (1987).

104. W. A. Fowler, *Nature*, 339, 345 (1989).

105. J. C. Jackson, *Nature*, 339, 345 (1989).

106. D. Lindley, *Nature*, 339, 567 (1989).

107. R. D. Petasso, X. Chen, K. W. Wenzel, R. R. Parker, C. K. Li, and C. Fiore, *Nature*, 339, 669 (1989).

108. D. E. Williams, D. J. S. Findlay, D. H. Craston, M. R. Sene, M. Bailey, S. Croft, B. W. Hooton, C. P. Jones, A. R. J. Kucernak, J. A. Mason, and R. I. Taylor, *Nature*, 342, 375 (1989).

109. J. S. Cohen and J. D. Davies, *Nature*, 342, 488 (1989).

Synthesis and X-ray Crystallographic Characterization of Spiro Orthocarbonates

Young Ja Park*, Kwang Hyun No, Ju Hee Kim, and Il-Hwan Suh[†]

Department of Chemistry, Sook Myung Women's University, Seoul 140-742

[†]*Department of Physics, College of Natural Sciences, Chungnam National University, Taejon 305-765*

Received January 22, 1992

In this study we have synthesized two spiro orthocarbonates, which can be polymerized with volume expansion, and determined their crystal structures. The crystal data are as follows: 3,4,10,11-Di(9,10-dihydro-9,10-ethanoanthracenyl)-1,6,8,13-tetraoxa-6,6-tridecane 5: $a = 16.898$ (1), $b = 9.299$ (1), $c = 24.359$ (2) Å, $\beta = 123.73$ (7)°, space group $P2_1/c$ and $R = 0.073$ for 2954 reflections; compound 8: $a = 15.244$ (4), $b = 15.293$ (3), $c = 10.772$ (3) Å, $\beta = 99.45$ (2)°, space group $P2_1/c$ and $R = 0.082$ for 2346 reflections. The seven-membered rings of compound 5 are chair forms and all the six-membered rings are boat shaped. For a six-membered spiro orthocarbonate, 3,9-Di(9-fluorenylidenyl)-1,4,6,9-tetraoxa-5,5-undecane 8, fluorene groups [C(1) atom through C(13) atom] are planar within ± 0.09 Å and the six-membered rings have chair conformations. The whole molecule has pseudo-C_2 symmetry. The water molecules in the crystal are linked with each other through the hydrogen bond with distance of 2.790 (20) Å.

Introduction

Monomers that will polymerize with no shrinkage or volume expansion are highly desirable for practical applications of polymeric materials, such as strain free composites, precision castings, dental filling and semi-conductor encapsulations. Spiro orthocarbonate, which is a bicycle compound, was found to expand volume on ring opening polymerization in which for every bond that goes from a van der Waals' distance to a covalent distance, at least two bonds would go from a covalent distance to a near van der Waals' distance. Therefore the volume shrinkage on a bond formation can be compensated with the volume expansion on two bonds breakage.

Baily and coworkers[1-3] reported the preparation of various spiro orthocarbonates and the practical applications such as in epoxy resin modifier, dental filling and elastomers. We also prepared several spiro orthocarbonates which have bulk and rigid side groups such as anthracene, naphthalene and benzene rings[4-6]. Here we report the syntheses of two spiro orthocarbonates and their crystal structures determined by single crystal X-ray diffraction method.
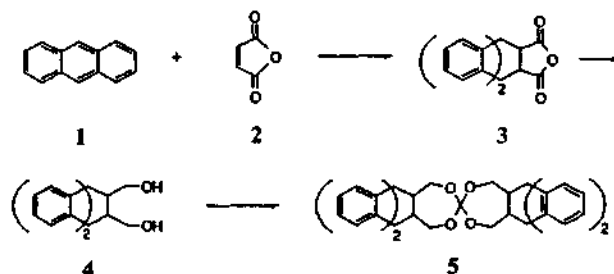

Figure 1. The synthesis of spiro orthocarbonate based on anthracene

Synthesis

In this study we have synthesized two new spiro orthocarbonates 5 and 8 as shown in Figures 1 and 2. The Diels-Alder adduct 3 was prepared in 91% yield from the reaction of anthracene and maleic anhydride in benzene· following the published procedure[7]. The diol 4 was first prepared in 80% yield by treatment of compound 3 with BF_3/$NaBH_4$ in diglyme[8]. However it has been found that this reaction can